

Title	Anomalous mechanical anisotropy of form polypropylene sheet with N,N -dicyclohexyl-2,6-naphthalenedicarboxamide
Author(s)	Phulkerd, Panitha; Nobukawa, Shogo; Uchiyama, Yohei; Yamaguchi, Masayuki
Citation	Polymer, 52(21): 4867-4872
Issue Date	2011-08-25
Type	Journal Article
Text version	author
URL	<a href="http://hdl.handle.net/10119/10729">http://hdl.handle.net/10119/10729</a>
Rights	NOTICE: This is the author's version of a work accepted for publication by Elsevier. Panitha Phulkerd, Shogo Nobukawa, Yohei Uchiyama, Masayuki Yamaguchi, Polymer, 52(21), 2011, 4867-4872, <a href="http://dx.doi.org/10.1016/j.polymer.2011.08.014">http://dx.doi.org/10.1016/j.polymer.2011.08.014</a>
Description	

**Anomalous Mechanical Anisotropy  
of  $\beta$  Form Polypropylene Sheet  
with *N,N'*-dicyclohexyl-2,6-naphthalenedicarboxamide**

Panitha Phulkerd,<sup>1</sup> Shogo Nobukawa,<sup>1</sup> Yohei Uchiyama,<sup>2</sup> and  
Masayuki Yamaguchi<sup>1\*</sup>

1) School of Materials Science,

Japan Advanced Institute of Science and Technology

1-1 Asahidai, Nomi, Ishikawa 923-1292 JAPAN

2) New Japan Chemical Co., Ltd.

13 Yoshijima, Yaguracho, Fushimi, Kyoto 612-8224, JAPAN

---

\* Corresponding to

Masayuki Yamaguchi

School of Materials Science, Japan Advanced Institute of Science and Technology

1-1 Asahidai, Nomi, Ishikawa 923-1292 Japan

Phone +81-761-51-1621, Fax +81-761-51-1625

E-mail m\_yama@jaist.ac.jp

**Abstract**

An extruded polypropylene (PP) sheet in which both the chain-axes of the PP molecules and the crystalline lamellae are oriented perpendicular to the flow direction is obtained via row-nucleation on a specific needle-shaped nucleating agent, *N,N'*-dicyclohexyl-2,6-naphthalenedicarboxamide. The sheet shows anomalous anisotropy in dynamic tensile modulus, in which, at lower temperatures, the storage modulus in the machine direction (MD) is lower than that in the transverse direction (TD), and this behavior reverses at high temperature. Tensile tests reveal that the Young's modulus and yield stress in the MD are higher than those in the TD. At high strain rate, the strain at break in the TD is, in contrast, markedly larger than that in the MD.

**Keywords:** polypropylene; molecular orientation; T-die extrusion; mechanical anisotropy

## Introduction

It is of great technological importance to control the crystalline structure of semi-crystalline polymers because it dominates the physical and chemical properties of the final products. In case of isotactic polypropylene (PP), the crystalline form must be examined in detail because PP is a polymorphic material with several modifications including  $\alpha$  monoclinic,  $\beta$  trigonal, and  $\gamma$  orthorhombic forms. In terms of mechanical properties, it is widely accepted that a high content of  $\beta$  form crystals is desired to achieve pronounced toughness,<sup>1-6</sup> which is one of the most important properties for PP. Therefore, substantial scientific and industrial effort has been directed towards increasing the content of  $\beta$  form crystals. In general, high content of  $\beta$  form crystals is obtained only through adopting suitable conditions such as addition of  $\beta$  nucleating agents and controlled processing conditions.<sup>5-8</sup> As well as the crystalline form, molecular orientation has a strong impact on the mechanical properties. It has been recognized that oriented semi-crystalline polymers show unique anisotropy in their dynamic mechanical properties,<sup>6,9-11</sup> as firstly demonstrated by Takayanagi et al.,<sup>11</sup> who found that the tensile modulus in the machine, i.e., oriented direction (MD) is higher than that in the transverse direction (TD) in the low temperature region, and that this behavior reverses at high temperature. Moreover, the mechanical responses including tensile anisotropy under large deformation depend strongly on both the molecular orientation as well as the crystalline form.

The deformation mechanism of  $\beta$  form PP has been studied, with a particular focus on the mechanical toughness. The most famous concept discussed was the idea of an energy dissipation process at the phase transformation from  $\beta$  to  $\alpha$  form crystals

during yielding; this concept successfully explained the ductile properties of  $\beta$  form PP.<sup>2-4</sup>

Chu et al. revealed that microvoid (crazes and/or small cracks) formation is dominant during plastic deformation of  $\beta$  form PP.<sup>12,13</sup> They discussed the mechanism based on the phase transformation. Since the density of  $\alpha$  form crystals or smectic form is higher than that of  $\beta$  form crystals, a volume contraction of the crystalline phase occurs during yielding, which leads to microvoid formation. Recently, a similar phenomenon was reported in  $\alpha$  form PP after removal of impurities and low molecular weight fraction; this was explained by the large amount of free volume in the amorphous region.<sup>14</sup> Li et al. examined the morphology of deformed PP by electron microscopy and found that unzipping deformation of lamellar stacks accompanied with microvoid formation occurred in  $\beta$  form PP.<sup>15,16</sup> Besides the void-opening process, lamellar fragmentation also occurs during yielding. According to rheo-optical studies by Huy et al.,<sup>17</sup> interlamellar slip and lamellar twisting are the major deformation mechanisms for  $\beta$  form PP. Lezak et al. demonstrated that interlamellar slip occurs in  $\beta$  form PP, using X-ray diffraction (XRD) measurements.<sup>18</sup> Finally, Luo et al. demonstrated that sufficient connection between crystallites, i.e., a large amount of tie molecules, is required for marked toughness to be exhibited, even in  $\beta$  form PP.<sup>19</sup>

Meanwhile, our research group successfully employed a new type of  $\beta$  nucleating agent, *N,N'*-dicyclohexyl-2,6-naphthalenedicarboxamide, to prepare PP sheets in which the chain axis (c-axis) of PP is oriented perpendicular to the flow direction.<sup>7,8,20,21</sup> The nucleating agent exists as needle-shaped crystals in molten PP; these crystals are oriented to the flow direction during extrusion processing by the hydrodynamic force. Then, PP molecules crystallize on the surface of the nucleating

agent; the growth direction of lamellae is perpendicular to the long axis of the needle-shaped nucleating agent. Furthermore, the c-axis of the PP crystals also orients perpendicular to the long axis of the needle crystals, as verified by infra-red dichroism and XRD.<sup>7,8</sup> A schematic illustration of the crystalline structure of PP on the needle-shaped nucleating agent is shown in Fig. 1. Although there are a lot of nucleating agents with fibrous or needle shapes,<sup>21-26</sup> this type of crystal growth has not yet been reported to the best of our knowledge. For blends with other anisotropic nucleating agents, a high level of molecular orientation to the flow direction has always been observed.<sup>21-26</sup>

[Fig. 1]

Since the direction of the molecular orientation is anomalous, it is expected that the mechanical anisotropy will also be different from that of a conventional extruded sheet, in which molecules orient to the flow direction.

In this study, the anisotropy of dynamic mechanical properties and tensile properties of an extruded sheet with anomalous molecular orientation is investigated in detail. The results obtained are discussed in terms of a mechanical model.

## Experimental

### Materials

A commercially available propylene homopolymer (SunAllomer, PM600A, Mn=63,000 and Mw=360,000) was used as the PP in this study. Further, *N,N'*-dicyclohexyl-2,6-naphthalenedicarboxamide (New Japan Chemical, NJ Star<sup>TR</sup> NU-100) was employed as a  $\beta$  nucleating agent. Mixing of PP with 0.1 wt% of the

nucleating agent was performed at 260 °C by a counter-rotating twin-screw extruder (Technovel, KZW 15TW-45 MG-NH rotation) at a screw rotation speed of 250 rpm. The pellets obtained were fed into a single-screw extruder equipped with a T-die (Tanabe-plastics, US25-28), 220 mm wide and with a 0.35 mm die lip. The out-put rate was 2 kg h<sup>-1</sup>. Then the sheet was stretched at 0.86 m min<sup>-1</sup> in the air gap between the die lip and the chill roll to adjust the thickness, 200 µm. The temperature of the die was controlled at 200 °C and the chill roll at 120 °C. A sheet of pure PP without the nucleating agent was also prepared using the same conditions as a reference sample.

The shear rate ( $\dot{\gamma}$ ) in the rectangular die was calculated to be 160 s<sup>-1</sup> by the following equation:<sup>27</sup>

$$\dot{\gamma} = \frac{6Q}{H^2W} \quad (1)$$

where  $Q$  is the volumetric flow rate, and  $H$  and  $W$  are the channel height and width, respectively. Furthermore, an average value of elongational strain rate was calculated by the following relation:

$$\dot{\epsilon} = \frac{v_1 v_2}{G} \quad (2)$$

where  $v_1$  and  $v_2$  are the average velocities of the sheet at the die exit and the chill roll, respectively, and  $G$  is the length of the air gap (30 mm). The elongational strain rate was roughly estimated to be 0.27 s<sup>-1</sup>.

## Measurements

The density of extruded sheet samples was measured with a top-loading electronic balance, using a flotation method.

Thermal analysis was conducted with a differential scanning calorimeter (Mettler, DSC820) under a nitrogen atmosphere to avoid thermal-oxidative degradation. Samples of approximately 10 mg in weight were sealed in aluminum pans. Melting profiles were recorded at a heating rate of  $10\text{ }^{\circ}\text{C min}^{-1}$ .

XRD measurements were carried out in reflection mode at room temperature using an X-ray diffractometer (Rigaku, Rint2500). The sheets were mounted directly into the diffractometer, such that the machine direction of the samples coincided with the main X-ray apparatus axis. The experiments were carried out using Cu-K $\alpha$  radiation operating at 40 kV and 30 mA at a scanning rate of  $1^{\circ}\text{ min}^{-1}$  over the diffraction angle  $2\theta$  (Bragg angle) range from  $10^{\circ}$  to  $30^{\circ}$ .

The molecular orientation of the extruded sheets was evaluated by infrared (IR) dichroism using a Fourier-transform infrared spectrometer (JASCO, FT-IR 6100) equipped with a polarizer. The absorbances of the bands at 841 and  $973\text{ cm}^{-1}$  were measured using a linearly polarized IR beam; the electric vector of the beam was positioned either parallel  $A_{//}$  or perpendicular  $A_{\perp}$  to the flow direction.<sup>10,28-30</sup> The  $841\text{ cm}^{-1}$  band is associated with the CH<sub>3</sub> rocking mode coupled with the C-CH<sub>3</sub> stretching mode in the crystalline phase. The  $973\text{ cm}^{-1}$  band is related to the rocking mode of CH<sub>3</sub> coupled with stretching of C-C in helical sequences, 5 units in length, in the amorphous phase.

The steady-state shear viscosity was measured using a cone-and-plate rheometer (Rheometric Scientific, Dynamic Stress Rheometer AR-2000) at  $200\text{ }^{\circ}\text{C}$  as a function of shear rate under a nitrogen atmosphere.

The temperature dependence of the dynamic tensile moduli was measured from  $-100$  to  $165\text{ }^{\circ}\text{C}$  using a dynamic mechanical analyzer (UBM, DVE V-4). The frequency

used was 10 Hz, and the heating rate was  $2\text{ }^{\circ}\text{C min}^{-1}$ . Rectangular specimens, 5 mm wide and 20 mm long, were cut out from the extruded sheet. In order to examine the mechanical anisotropy, two types of samples were prepared: one was parallel to the flow direction (MD sample) and the other was perpendicular to the flow direction (TD sample). Therefore, in the case of the MD sample, the direction of the oscillatory strain applied coincides with the flow direction.

Stress-strain behavior in uniaxial tension was measured using a tensile machine (Tokyo testing machine, SBR-500N) following ASTM D638 at room temperature. The sample specimens were cut out from the sheets with a razor blade following ASTM D-1822L. The initial distance between the gauges was 10 mm and one of them was moved at a constant speed of either 10 or 100  $\text{mm min}^{-1}$ . All measurements were performed at least ten times, and the average values were calculated. The elongation at the break point was evaluated by measuring the final gauge length of the narrow part of the dumbbell.

## Results and Discussion

### Characterization of extruded sheet

Fig. 2 shows XRD patterns for the extruded sheets of PP and PP containing 0.1 wt% of the nucleating agent. In agreement with the results obtained in previous studies on sheets containing 0.05 wt% of the nucleating agent,<sup>7,8</sup> strong peaks are detected at  $2\theta = 16.1^{\circ}$  and  $21.0^{\circ}$ , and ascribed to  $\beta$  form crystals. The  $K$  values of PP and PP containing the nucleating agent are 0.18 and 0.97, respectively.

[Fig. 2]

The melting behavior of the sheets is shown in Fig. 3. As seen in the figure, the sheet of pure PP shows a distinct melting peak at 163 °C ascribed to  $\alpha$  form crystals with a weak shoulder peak at 143 °C from a small amount of  $\beta$  form crystals. In contrast, the extruded sheet containing the nucleating agent has intense double peaks at 150 and 169 °C, which were also detected in the previous paper.<sup>7</sup> Although the peak due to  $\alpha$  form crystals is detected in the DSC curve for the sheet containing the nucleating agent, they will be formed during the measurement after the  $\beta$  form crystals have melted. In general, the melting peak of  $\alpha$  form crystals obtained by rapid cooling appears at approximately 165 °C; the exact temperature depends on the melting and recrystallization processes during heating, along with the recrystallization rate and the scanning rate.<sup>31</sup> The high melting point of  $\alpha$  form crystals, detected in the present experiment, may be attributed to their crystallization from an ordered melt (i.e., the melting of  $\beta$  form crystals). As well known for PP, the lamellar thickness of  $\beta$  form crystals is much larger than that of  $\alpha$  form crystals,<sup>32,33</sup> which means that large regions of ordered melt will result from  $\beta$  form crystal melting. Consequently, thick lamellae of  $\alpha$  form crystals are generated during the heating process for the present sample. Similar phenomena have been reported by Cho et al.<sup>34</sup> and Liu et al.<sup>35</sup>

[Fig. 3]

Table 1 summarizes the heat of fusion for  $\alpha$  and  $\beta$  form crystals, along with the density data measured by the flotation method at room temperature. Because the crystal density of  $\beta$  form crystals is lower,<sup>1</sup> the sheet containing the nucleating agent shows slightly lower density.

[Table 1]

The molecular orientation of the extruded sheets is characterized by the

dichroic ratio  $D (\equiv A_{\parallel}/A_{\perp})$  of the infrared absorption peaks at 841 and 973  $\text{cm}^{-1}$ . The absorption peaks are ascribed to the crystalline (841  $\text{cm}^{-1}$ ) and amorphous (973  $\text{cm}^{-1}$ ) regions, respectively. The values of Hermans orientation function,  $F$ , were evaluated for both peaks assuming the electric vector is parallel to the MD,<sup>8,24</sup> and are shown in Table 1. Both orientation functions are almost unity for pure PP, indicating no molecular orientation. On the other hand, the orientation functions of the sheet containing the nucleating agent are -0.053 (crystal) and 0.007 (amorphous). This result demonstrates that PP chains in the crystals have oriented perpendicular to the flow direction. In contrast, the orientation function of amorphous chains is close to zero, i.e., their orientation is random, on average. However, the orientation condition of the amorphous chains must be able to be roughly classified into two types. Some amorphous parts will orient perpendicular to the flow direction, in accordance with the molecules in the crystals, because of their connection to crystals. The other parts, which are separated from the crystals, can adopt an orientation independent of the crystalline phase. Considering that the former chains must have a negative orientation function (similar to the chains in the crystals), the other independent amorphous chains must possess a positive orientation function, presumably due to the hydrodynamic force during processing. In fact, PP employed in this study shows shear thinning behavior even at 0.1  $\text{s}^{-1}$  at 200 °C, suggesting that a high level of molecular orientation is attained at the die exit (160  $\text{s}^{-1}$ ). The prompt solidification by the nucleating agent could fix the amorphous chains in this deformed state. As a result, the orientation of the amorphous chain is, on average, cancelled out.

[Table 1]

### Dynamic mechanical properties

As demonstrated in our preceding papers,<sup>7,8</sup> MD and TD samples show almost the same dynamic mechanical spectra for pure PP. Therefore, the crossing behavior of dynamic moduli is not observed. This is reasonable because pure PP shows weak or no molecular orientation owing to its slow crystallization, which allows orientational relaxation. However, for the sheet containing the nucleating agents, the magnitude of  $E'$  in the MD is lower than that in the TD in the low temperature region, and reverses at high temperature, as seen in Fig. 4. A similar phenomenon was reported for injection-molded PP,<sup>29,30,36,37</sup> although the order of the modulus was completely opposite to the present result. Moreover, it should be noted that the crossing behavior for the present sample is more pronounced than that for injection-molded products with high level of molecular orientation.<sup>29,37</sup>

[Fig. 4]

The crossing behavior was explained by a mechanical model, the Takayanagi model, as illustrated in Fig. 5, in which the oriented crystalline phase shows strong anisotropy in modulus.<sup>11,36,38</sup> The parameters  $\lambda$  and  $\phi$  represent the degrees of connection of the crystalline phase in direction 2 and direction 1, respectively. Therefore, the value of  $(1-\lambda)(1-\phi)$  is the volume fraction of amorphous phase. For a product obtained by a conventional processing operation, direction 1 is the flow direction, i.e., MD. In this case, the crossing behavior is detected when  $\phi$  is considerably larger than  $\lambda$ . It is generally recognized that the skin layer in injection-molded PP is composed of “shish-kebab” structures, in which the axis of the “shish” aligns parallel to the flow direction. The shish acts as nucleating templates, leading to folded-chain lamellae, the “kebab”, oriented perpendicular to the flow direction.<sup>10,38</sup> The crossing behavior in the

dynamic moduli can be explained by a shish-kebab structure with a large amount of kebab.

In the present sample, direction 2 is the flow direction. Therefore, the crossing behavior in Fig. 4 demonstrates that  $\phi$  is larger than  $\lambda$ . Moreover, Fig. 4 shows that the peak area of  $E''$ , ascribed to the glass-to-rubber transition, is smaller in the MD than that in the TD. This result is consistent with  $\phi > \lambda$ . Considering that both lamellae and chains in crystals do not orient to the flow direction, a lot of amorphous chains deformed by hydrodynamic force during extrusion will act as tie molecules between crystallites in the flow direction as suggested by the orientation function. In other words, the anisotropy of the tie molecule fraction is responsible for the peculiar dynamic mechanical properties. This is reasonable because tie molecules, defined as amorphous chains which connect neighboring crystals, greatly affect the mechanical properties in the solid state.<sup>19,29,39-42</sup> In the current experiment, the amount of series connections in the lamellae aligned to the flow direction increases presumably owing to the deformed amorphous molecules after extrusion from the die.

The anomalous dynamic mechanical properties could be pronounced at high out-put rate, because the deformation of the PP chains towards the flow direction will be greater. The small lateral size and large lamellar thickness of  $\beta$  form crystals, as demonstrated by Kotek et al.,<sup>33</sup> could be also responsible for the anisotropy in the tie molecule fraction.

[Fig. 5]

The effect of the tensile direction on the stress-strain curves at room temperature is shown in Figs. 6 and 7 at strain rates of  $0.017 \text{ s}^{-1}$  and  $0.17 \text{ s}^{-1}$ . The tensile

properties of the extruded sheets, such as yield stress, strain at the yield point, stress at break, and strain at break at low and high strain rates, are summarized in Table 2.

[Table 2]

Stress-strain curves of PP with  $\beta$  form crystals have been widely studied by means of rheo-optical measurements,<sup>17</sup> XRD measurements,<sup>18,42-22</sup> electron microscope observations<sup>12-16</sup> and so on, and clarified in detail as summarized in the introduction. Moreover, the tensile properties of oriented  $\beta$  form PP (mainly prepared by injection-molding) have been studied and marked toughness has been found.<sup>33,44-50</sup> However, the anisotropy in the stress-strain curves has not been studied in these previous reports.

As seen in the figures, the PP sheet shows brittle behavior irrespective of the tensile direction and the strain rate in our experimental range. The highest yield stress is detected in MD stretching at  $0.17 \text{ s}^{-1}$ . Compared to the pure PP, ductile behavior is clearly detected for PP containing the nucleating agent. This result has been reported by many researchers.<sup>33,44-50</sup>

[Fig. 6]

Distinct differences in the tensile behavior between MD and TD samples are detected for the sheet containing the nucleating agent, especially at the high strain rate (Fig.7). At the low strain rate, the initial slope of the stress, i.e., Young's modulus, for the TD sample is comparatively lower than that for the MD sample, although both lamellae and chains in crystals are oriented perpendicular to the flow direction. This is a similar phenomenon to that observed in the dynamic mechanical properties. Since the strains at the yield point are almost the same, the yield stress in MD stretching is higher. Moreover, the strain at break in TD is obviously larger than that in MD at the high

strain rate. Even at the low strain rate, approximately one-third of the samples showed brittle behavior in MD stretching (more than 10 specimens were stretched at the same conditions for each sample), whereas ductile deformation was always detected in TD stretching.

[Fig. 7]

For the sample containing the nucleating agent, it was expected that the yield stress in the TD would be higher than that in the MD, because fragmentation of the lamellae cannot be avoided in TD stretching even under a small strain. However, higher yield stress was detected in MD stretching, although both lamellae and chains in the crystals do not exist continuously in this direction. These tensile results can be explained by the large number of amorphous chains connecting neighboring lamellae along the flow direction, i.e., the tie molecules. This is reasonable considering the recent work by Luo et al. on the relation between tie molecules and the deformation mechanism of  $\beta$  form PP.<sup>19</sup>

Fig. 8 shows stress-whitening behavior during stretching. It should be noted that inhomogeneous localized deformation occurs with intense stress-whitening during MD stretching of the sheet containing the nucleating agent. Considering the structure of the extruded sheet, unzipping of lamellar stacks accompanied with generation of microvoids would dominate the deformation. The localized deformation develops into a necking band, which can be clearly detected beyond the yield point. After the necking region extends to most of the narrow parts of the dumbbell, the stress increases again with strain, probably due to the formation of fibril structure, until final rupture. In contrast, the necking deformation is not detected in TD stretching and stress-whitening appears homogeneously in the narrow part of the dumbbell specimens. Homogeneous

stress-whitening is also detected for the PP sheet in both MD and TD stretchings.

Li et al. suggested that the separation of neighboring lamellae mainly occurs when the lamellae orient perpendicular to the loading direction, leading to the deformation bands.<sup>51</sup> On further loading, these deformation bands develop into crazes and cracks. In the current experiments, numerous cracks oriented perpendicular to the stretching direction appear on the surface in MD stretching for PP containing the nucleating agent (not shown here). Because of the distinct yield point, along with the perpendicular cracks, some samples show brittle fracture in MD stretching, which could be explained by Considère's construction.<sup>38</sup> On the contrary, there are no cracks on the surface of TD samples containing the nucleating agent during the formation of a necking region. Consequently, samples produce a stable necking band in TD stretching, whereas one-third of the samples exhibited brittle behavior in MD stretching. Once the stress-whitening region extends, even the MD sample shows ductile deformation.

[Fig. 8]

## Conclusion

The relationship between the structure and the mechanical properties of extruded sheets of PP containing *N,N'*-dicyclohexyl-2,6-naphthalenedicarboxamide as a  $\beta$  nucleating agent is studied. The sheet is found to contain a large amount of  $\beta$  form crystals. During DSC measurements, after the  $\beta$  form crystals have melted,  $\alpha$  form crystals with extraordinarily high melting point appear, as a result of recrystallization from a highly ordered melt.

PP molecules orient perpendicular to the flow direction in the sheet containing the nucleating agent. The crossing behavior of  $E'$  in MD and TD samples is detected

clearly around the glass transition temperature in spite of the low level of molecular orientation. Moreover, it is found from the tensile testing that the Young's modulus and yield stress in MD stretching are higher than those in TD. However, the sample shows brittle behavior in MD stretching especially at high strain rate, because of the generation of localized microvoids and surface cracks (voids without fibrils) with a distinct yield point. In contrast, ductile deformation with homogeneous stress-whitening is always detected in TD stretching.

The infrared dichroic ratios reveal that the Hermans orientation function of the amorphous phase is close to zero, whereas it has a negative value for PP chains in crystals in the sheet containing the nucleating agent. The low level of orientation function in the amorphous region is explained by the existence of molecules deformed to the flow direction by hydrodynamic force, which will connect the crystals along the flow direction, i.e., tie molecules. In other words, the anisotropy of the tie molecule fraction is responsible for the peculiar mechanical anisotropy in our PP samples containing the  $\beta$  nucleating agent.

## References

1. Phillips RA, Wolkowicz MD. Polypropylene Morphology. In: Nello P, editor. Polypropylene Handbook. Munich: Hanser; 2005. pp. 195-210.
2. Karger-Kocsis J, Varga J. J Appl Polym Sci 1996;62:291-300.
3. Karger-Kocsis J. Polym Bull 1996;36:119-24.
4. Karger-Kocsis J. Polym Eng Sci 1996;36:203-10.

5. Tjong SC. Deformation Behavior of  $\beta$ -Crystalline Phase Polypropylene and Its Rubber-Modified Blends. In: Nwabunma D, Kyu T, editors. Polyolefin Blends. New Jersey: Wiley; 2008. pp. 305-9.
6. Varga J. J Macromol Sci Phys 2002;B41:1121-71.
7. Uchiyama Y, Iwasaki S, Ueoka C, Fukui T, Yamaguchi M. J Polym Sci Polym Phys 2009;47:424-33.
8. Yamaguchi M, Fukui T, Okamoto K, Sasaki S, Uchiyama Y, Ueoka C. Polymer 2009;50:1497-504.
9. White JL, Choi DD. Polyolefins Processing, Structure Development, and Properties. Munich: Hanser; 2005. pp. 91-105.
10. Bower DI. Infrared dichroism, Polarized fluorescence and Raman spectroscopy. In: Ward IM, editor. Structure and Properties of Oriented Polymers. London: Chapman & Hall; 1997. pp. 181-233.
11. Takayanagi M, Imada K, Kajiyama T. J Polym Sci C 1960;15:263-81.
12. Chu F, Yamaoka T, Ito H, Kimura Y. Polymer 1994;35:3442-48.
13. Chu F, Yamaoka T, Kimura Y. Polymer 1995;36:2523-30.
14. Rozanski A, Galeski A, Debowska M. Macromolecules 2011;44:20-8.
15. Li JX, Cheung WL, Chan CM. Polymer 1999;40:2089-102.
16. Li JX, Cheung WL, Chan CM. Polymer 1999;40:3641-56.
17. Huy TA, Adhikari R, Lüpke T, Henning S, Michler GH. Polymer 2004;42:4478-88.
18. Lezak E, Bartczak Z, Galeski A. Polymer 2006;47:8562-74.
19. Luo F, Geng C, Wang K, Deng H, Chen F, Fu Q, Na B. Macromolecules 2009;42:9325-31.

20. Yamaguchi M, Irie Y, Phulkerd P, Hagihara H, Hirayama S, Sasaki S. *Polymer* 2010;51:5983-89.
21. Yamaguchi M. Material Design of High Performance Polypropylene Containing Nucleating Agent. In: Lechkov M, Prandzheva S, editors. *Encyclopedia of Polymer Composites*. New York: Nova Science Publishers; 2010. pp. 1043-58.
22. Kristiansen M, Tervoort T, Smith P. *Macromolecules* 2005;38:10461-65.
23. Tenma M, Yamaguchi M. *Polym Eng Sci* 2007;47:1441-46.
24. Tenma M, Mieda N, Takamatsu S, Yamaguchi M. *J Polym Sci Polym Phys* 2007;46:41-47.
25. Patil N, Balzano L, Portale G, Rastogi S. *Macromolecules* 2010;43:6749-59.
26. Phillips AW, Bhatia A, Zhu P, Edward G. *Macromolecules* 2011;44:3517-28.
27. Tadmor Z, Gogos CG. *Principles of Polymer Processing*, 2nd Ed. Wiley-Interscience, New York, 2006.
28. Onogi S, Asada T, Tanaka A. *J Polym Sci A* 1969;7:171-82.
29. Yamaguchi M, Suzuki K, Miyata H. *J Polym Sci Polym Phys* 1999;37:701-13.
30. Nitta K, Yamaguchi M. Deformation Behavior of  $\beta$ -Crystalline Phase Polypropylene and Its Rubber-Modified Blends. In: Nwabunma D, Kyu T, editors. *Polyolefin Blends*. New Jersey: Wiley; 2008. pp. 305-9.
31. Wtochowicz A, Eder M. *Polymer* 1984;25:1268-70.
32. Ullmann W, Wendorff JH. *Prog Colloid Polym Sci* 1979;66:25-33.
33. Koteck J, Raab M, Baldrian J, Grellmann W. *J Appl Polym Sci* 2002;85:1174-84.
34. Cho K, Saheb DN, Choi J, Yang H. *Polymer* 2002;43:1407-16.
35. Liu M, Guo B, Du M, Chen F, Jia D. *Polymer* 2009;50:3022-30.
36. Ferry JD. *Viscoelastic Properties of Polymers*. New York: Wiley; 1980. pp. 425-34.

37. Fujiyama M, Wakino T, Kawasaki Y. J Appl Polym Sci 1988;35:29-49.
38. Ward IM, Hadley DW. An Introduction to the Mechanical Properties of Solid Polymers. Chichester: Wiley; 1993. pp. 213-45.
39. Peterlin A. J Macromol Sci Phys 1972;B6:583-89.
40. Huang YL, Brown N. J Polym Sci Polym Phys 1991;29:129-37.
41. Strebel JJ, Moet A. J Polym Sci Polym Phys 1995;33:1969-84.
42. Asano T, Fujiwara Y. Polymer 1978;19:99-108.
43. Li JX, Cheung WL. Polymer 1998;39:6935-40.
44. Scudla J, Raab M, Eichhorn KJ, Strachota A. Polymer 2003;44:4655-64.
45. Scudla J, Eichhorn KJ, Raab M, Schmidt P, Jehnichen D, Häubler L. Macromol Symp 2002;184:371-87.
46. Raab M, Scudla J, Kolarik J. Eur Polym J 2004;40:1317-23.
47. Obadal M, Cermak R, Habrova V, Stoklasa K, Simonik J. Intern Polym Process 2004;19:308-12.
48. Kotek J, Kelner I, Baldrian J, Raab M. Eur Polym J 2004;40:2731-38.
49. Cermak R, Obadal M, Ponizil P, Polaskova M, Stoklasa K, Lengalova A. Eur Polym J 2005;41:1838-45.
50. Cermak R, Obadal M, Ponizil P, Polaskova M, Stoklasa K, Heckova J. Eur Polym J 2006;41:2185-91.
51. Li JX, Cheung WL, Ji D. Polymer 1999;40:1219-22.

**Figure Captions**

- Figure 1 Schematic illustration of PP crystals on a needle-shaped nucleating agent.
- Figure 2 XRD patterns of the extruded sheets for pure PP and PP with the nucleating agent (NA).
- Figure 3 DSC heating curves of the extruded sheet samples at a heating rate of  $10\text{ }^{\circ}\text{C min}^{-1}$ .
- Figure 4 Temperature dependence of tensile modulus such as  $E'$  (circles) and  $E''$  (diamonds) for an extruded sheet in MD (closed symbols) and TD (open symbols) directions for PP containing the nucleating agent.
- Figure 5 Mechanical model of oriented crystalline polymers. The dashed region represents crystalline phase in which the c-axis orients to the direction of the lines. The white region denotes amorphous phase.
- Figure 6 Stress-strain curves of pure PP in MD (black line) and TD (gray line) directions at different strain rates; (a)  $0.017\text{ s}^{-1}$  and (b)  $0.17\text{ s}^{-1}$ .
- Figure 7 Stress-strain curves of PP containing the nucleating agent in MD (black line) and TD (gray line) directions at different strain rates; (a)  $0.017\text{ s}^{-1}$  and (b)  $0.17\text{ s}^{-1}$ .
- Figure 8 Optical photographs of sample specimens after removal of the stress at various strains; (a) MD stretching for PP (b) TD stretching for PP, (c) MD stretching for PP containing the nucleating agent, and (d) TD stretching for PP containing the nucleating agent. The stretching rate was  $0.017\text{ s}^{-1}$ .

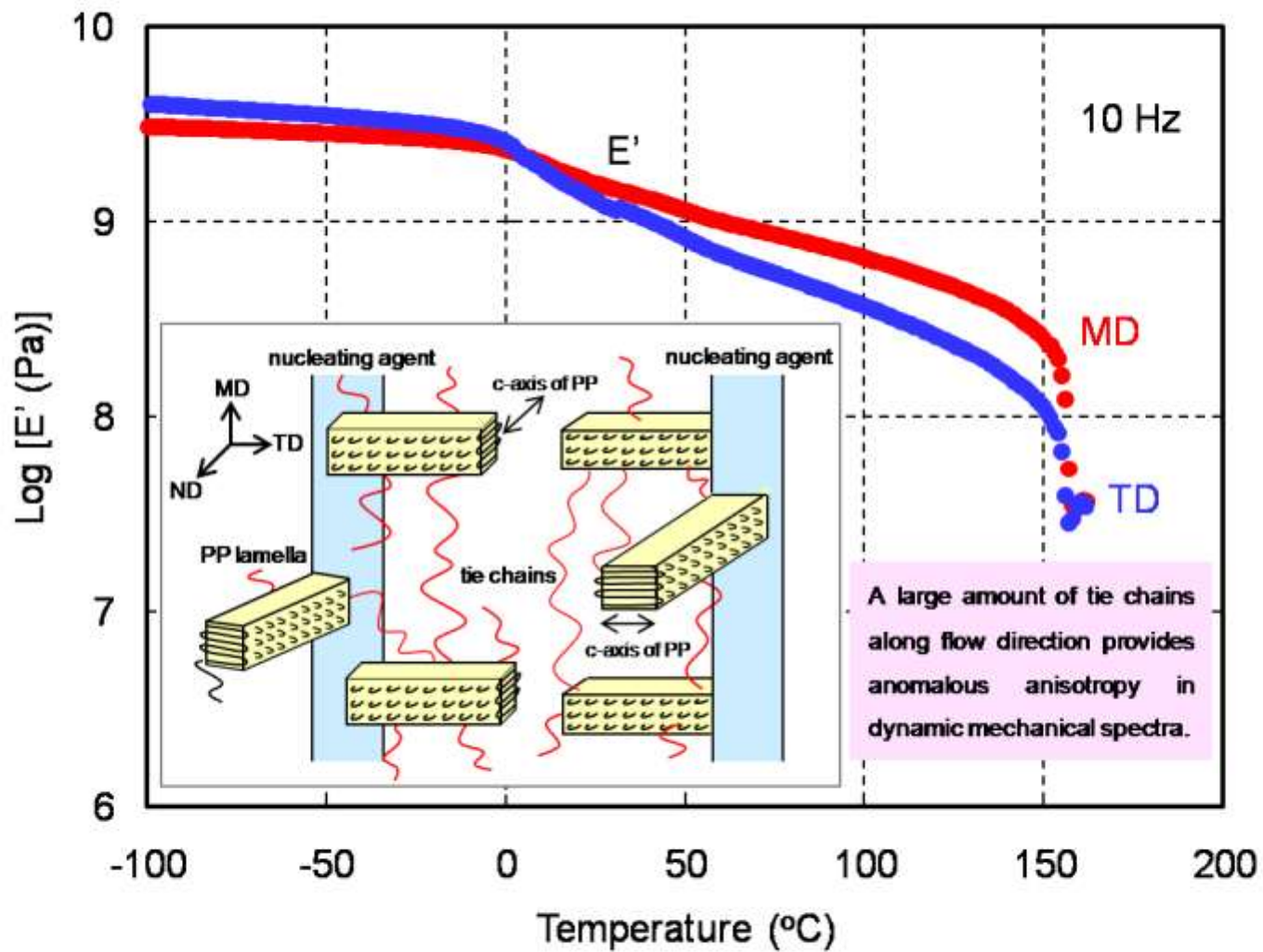


**Table 1 Characteristics of Sample Sheets**

Sample	Density (kg/m <sup>3</sup> )	Heat of Fusion (J/g)		Orientation Function, <i>F</i>	
		$\beta$ -form	$\alpha$ -form	841 (cm <sup>-1</sup> )	973 (cm <sup>-1</sup> )
PP	916	1.7	69.7	0.009	0.010
PP with NA	894	60.7	46.9	-0.053	0.007

**Table 2 Characteristics of Stress-Strain Behavior for Sample Sheets**

<b>Sample</b>	<b>Strain rate (s<sup>-1</sup>)</b>	<b>Drawing direction</b>	<b>Yield Stress (MPa)</b>	<b>Strain at Yield Point</b>	<b>Stress at Break (MPa)</b>	<b>Strain at Break</b>
<b>Pure PP</b>	<b>0.017</b>	<b>MD</b>	<b>33.8</b>	<b>0.099</b>	<b>31.5</b>	<b>0.31</b>
	<b>0.017</b>	<b>TD</b>	<b>34.1</b>	<b>0.108</b>	<b>31.0</b>	<b>0.27</b>
	<b>0.17</b>	<b>MD</b>	<b>37.5</b>	<b>0.123</b>	<b>36.0</b>	<b>0.21</b>
	<b>0.17</b>	<b>TD</b>	<b>33.6</b>	<b>0.105</b>	<b>35.1</b>	<b>0.16</b>
<b>PP with NA</b>	<b>0.017</b>	<b>MD</b>	<b>31.7</b>	<b>0.063</b>	<b>38.1</b>	<b>11.14</b>
	<b>0.017</b>	<b>TD</b>	<b>25.2</b>	<b>0.067</b>	<b>40.9</b>	<b>11.81</b>
	<b>0.17</b>	<b>MD</b>	<b>38.3</b>	<b>0.072</b>	<b>27.6</b>	<b>3.29</b>
	<b>0.17</b>	<b>TD</b>	<b>28.0</b>	<b>0.074</b>	<b>43.3</b>	<b>11.26</b>

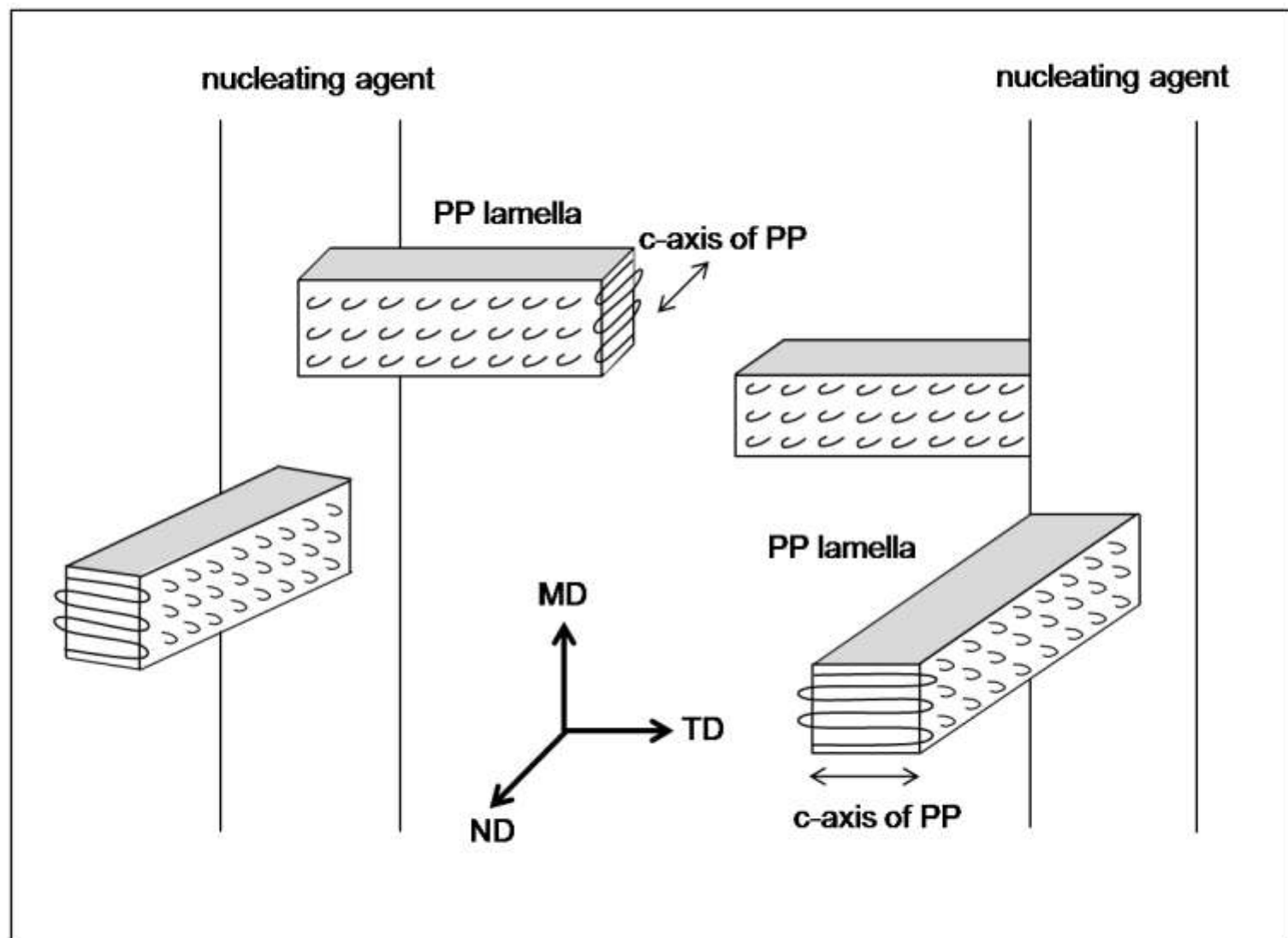


Figure 1

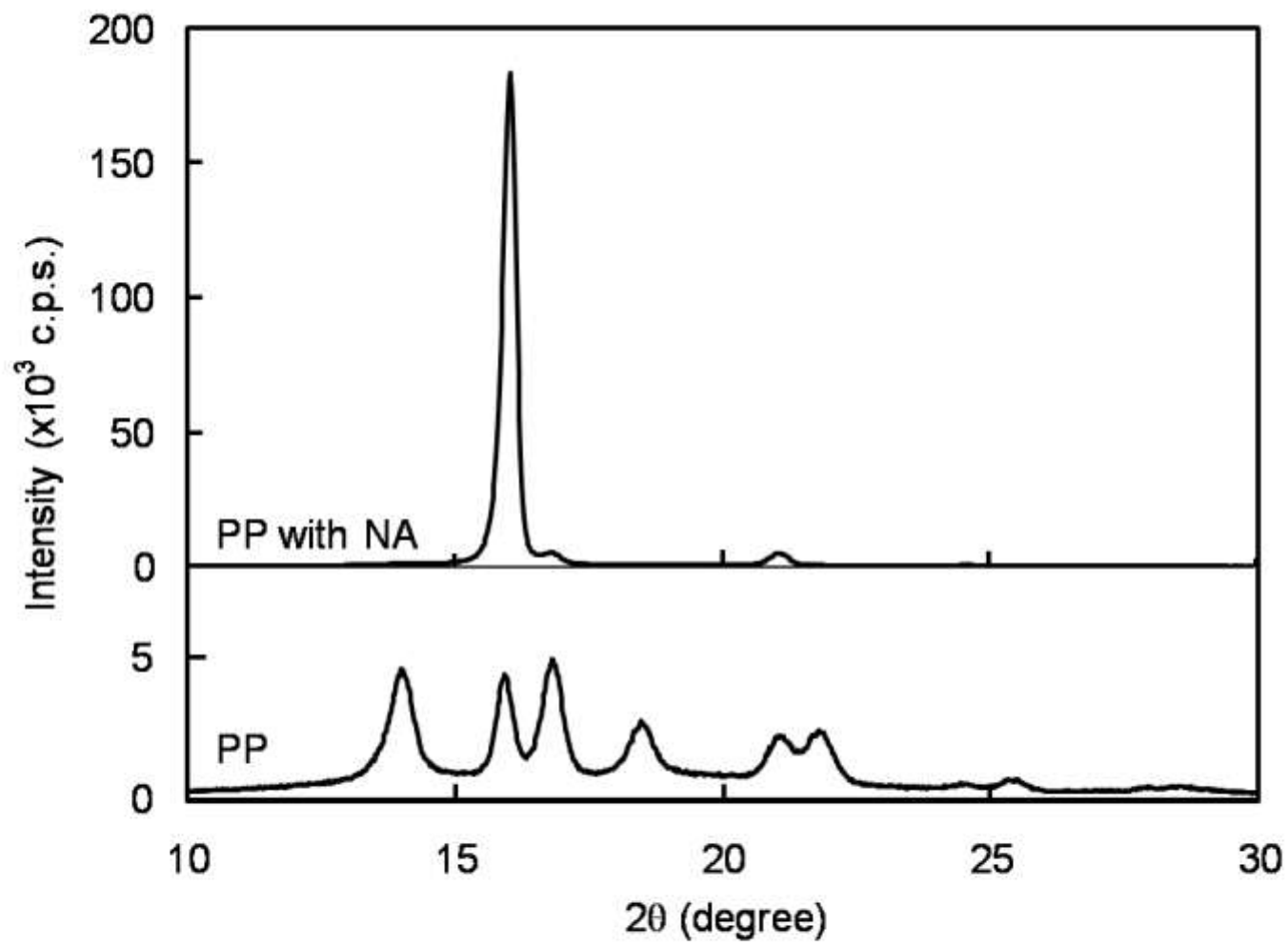


Figure 2

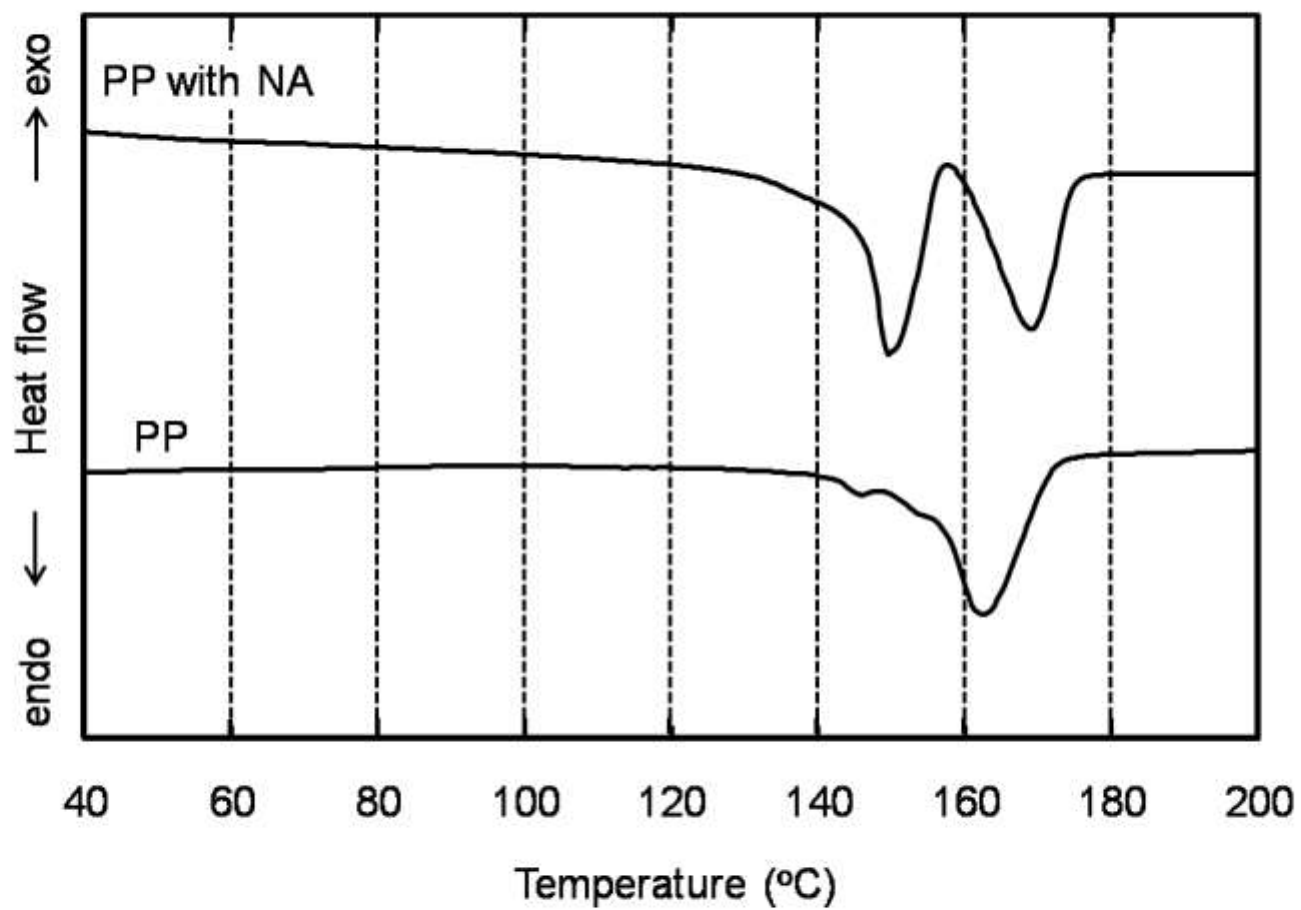


Figure 3

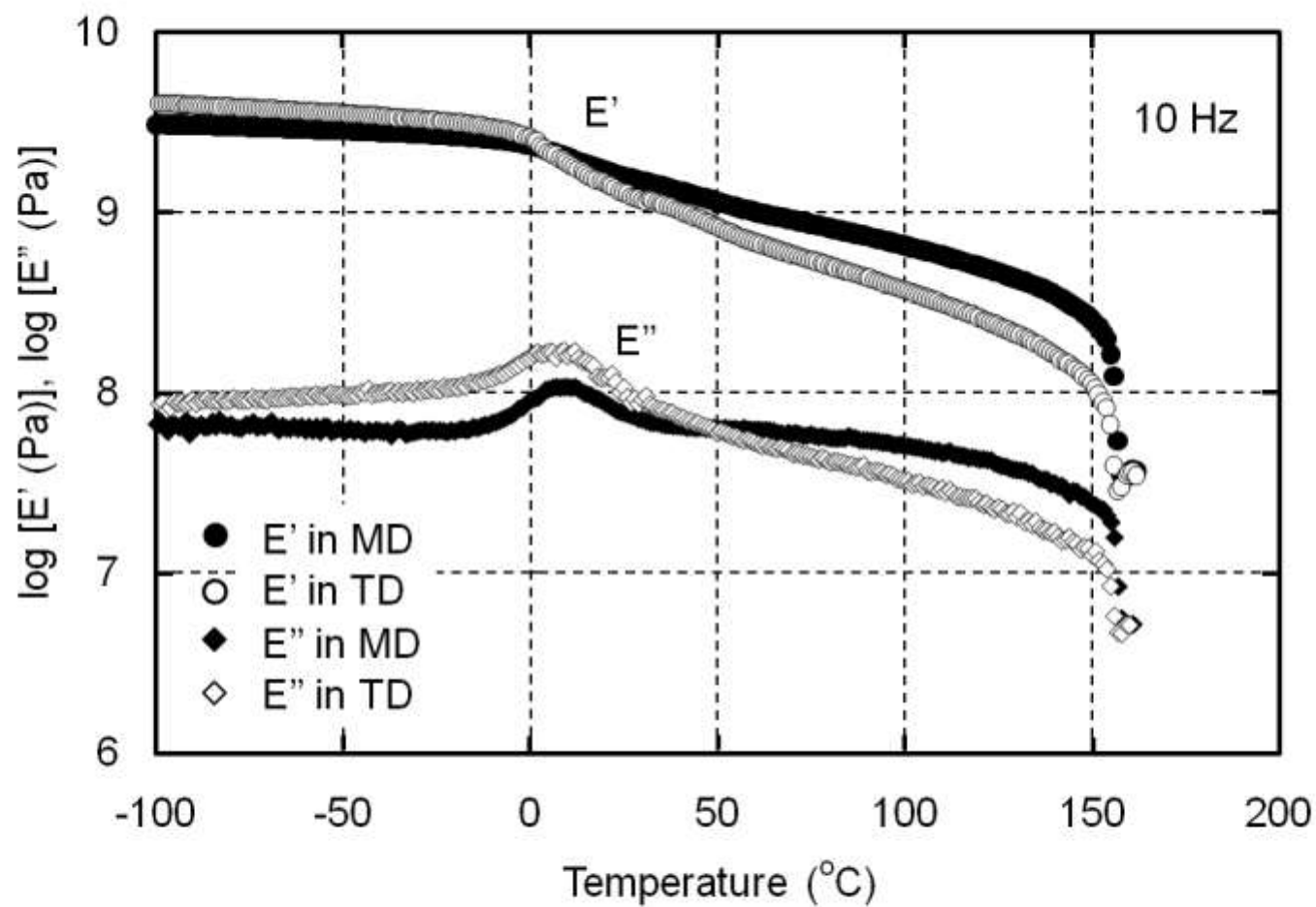


Figure 4

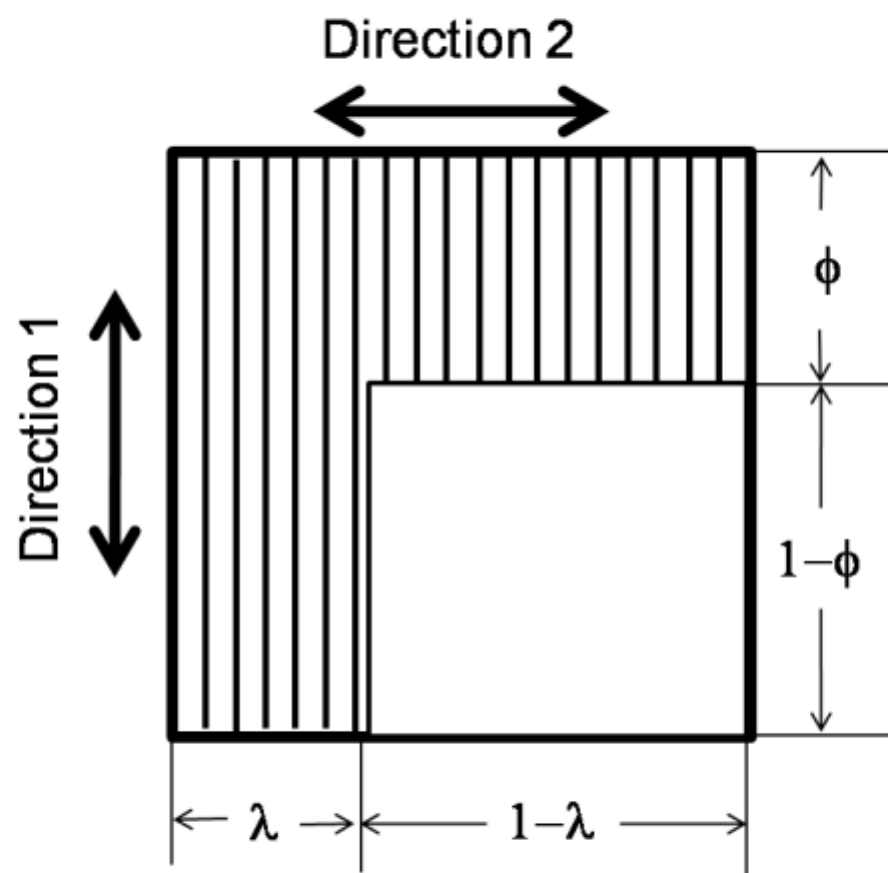


Figure 5

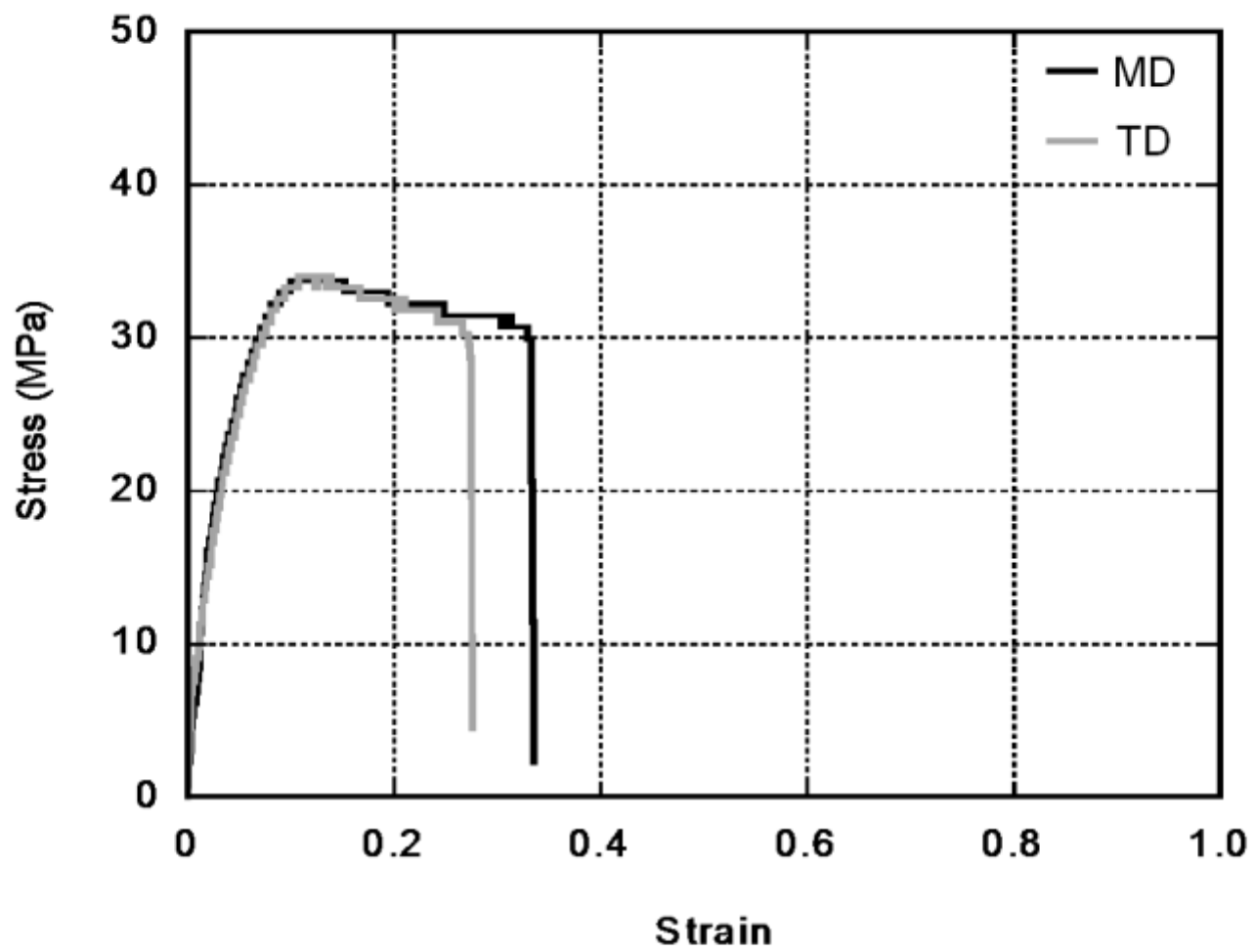


Figure 6 (a)

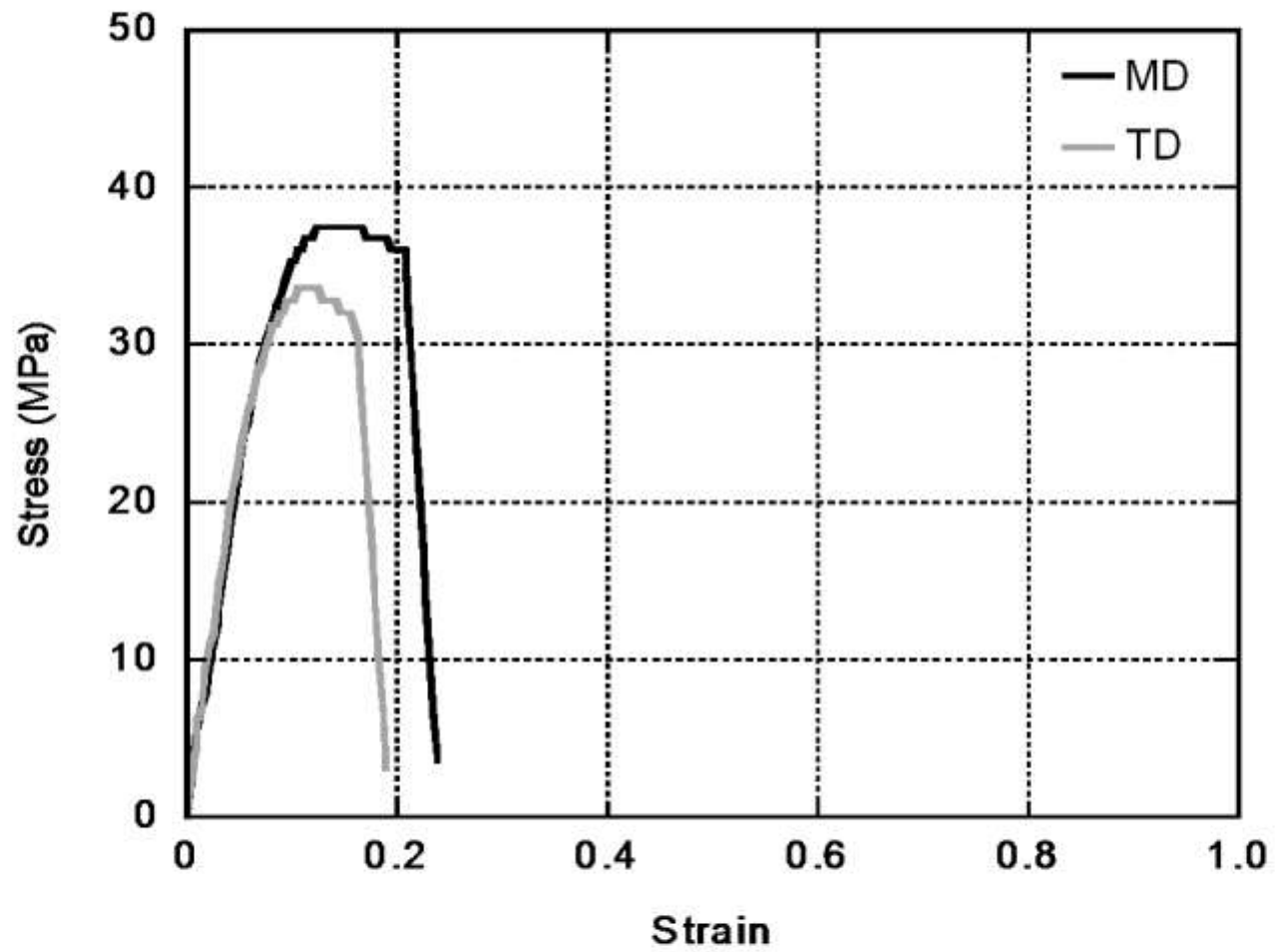


Figure 6 (b)

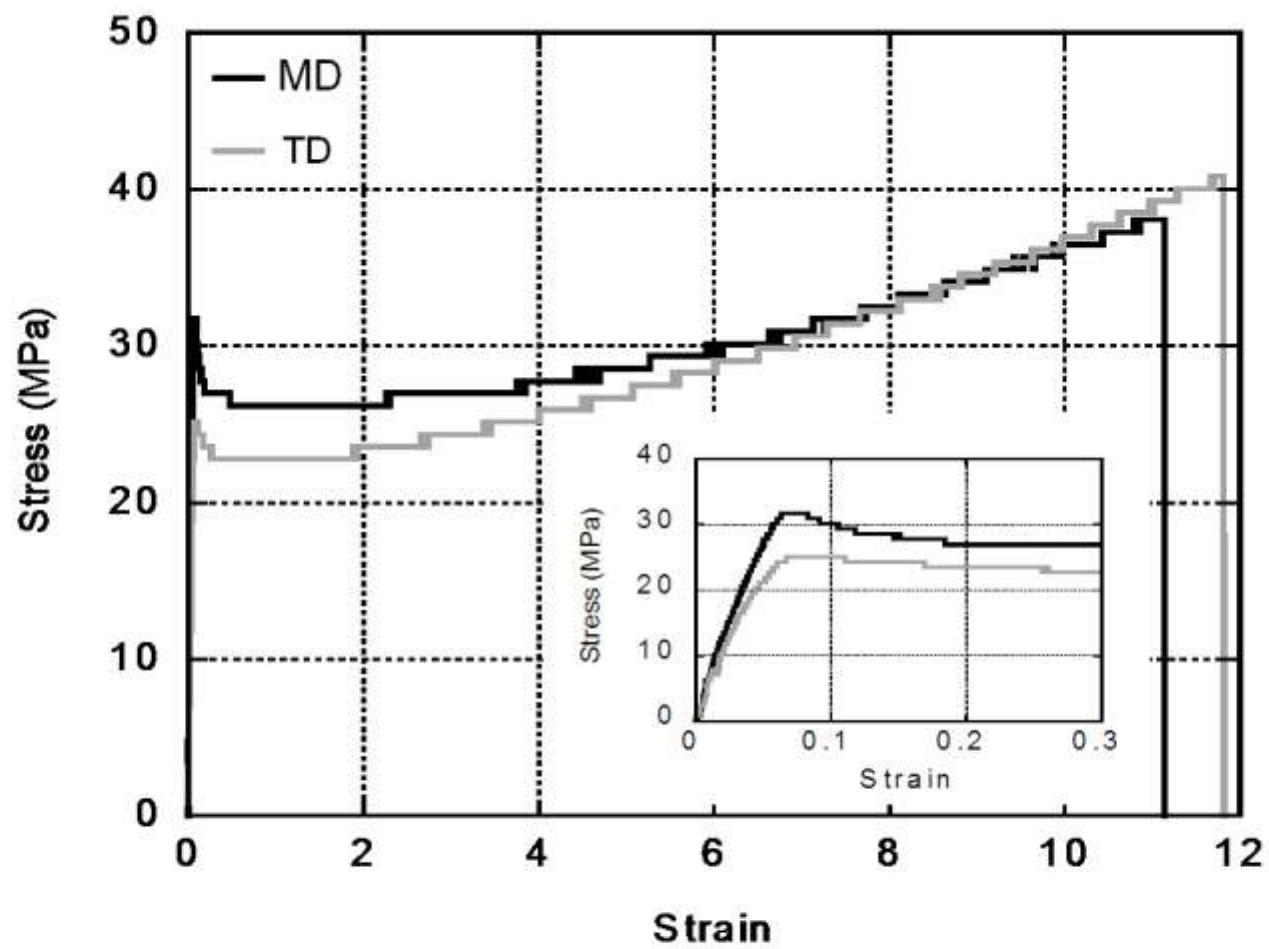


Figure 7 (a)

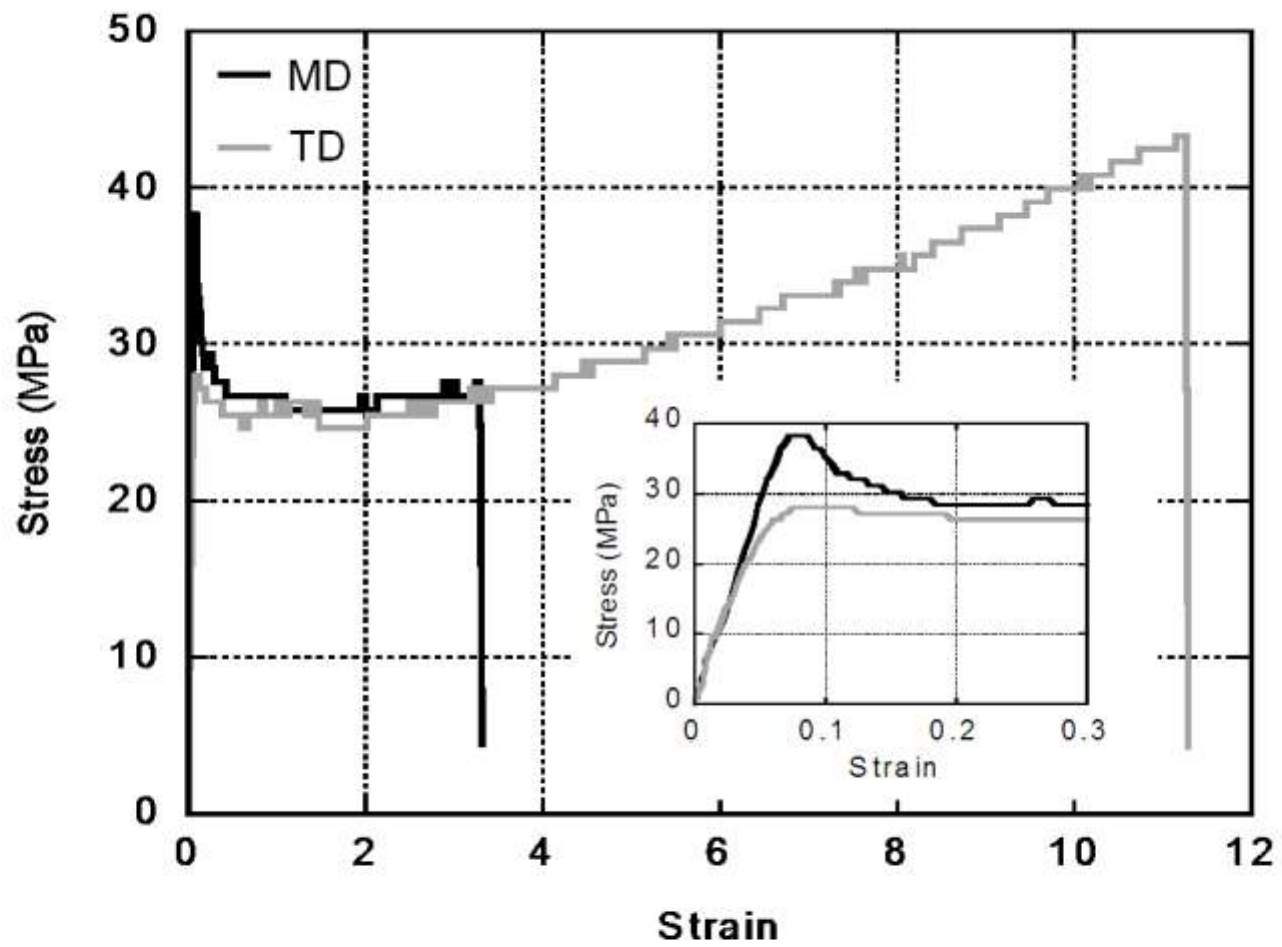


Figure 7 (b)

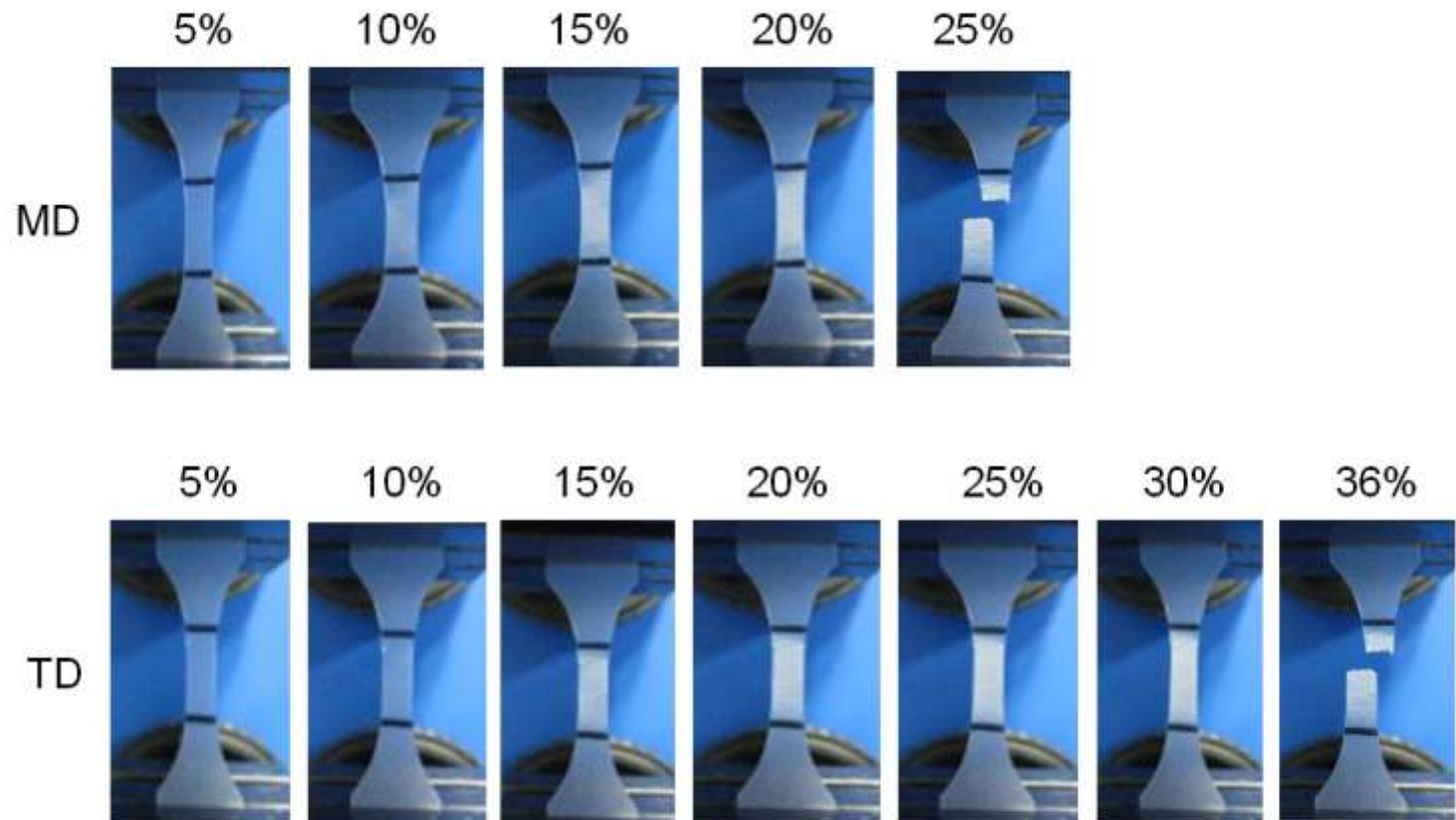


Figure 8 (a)

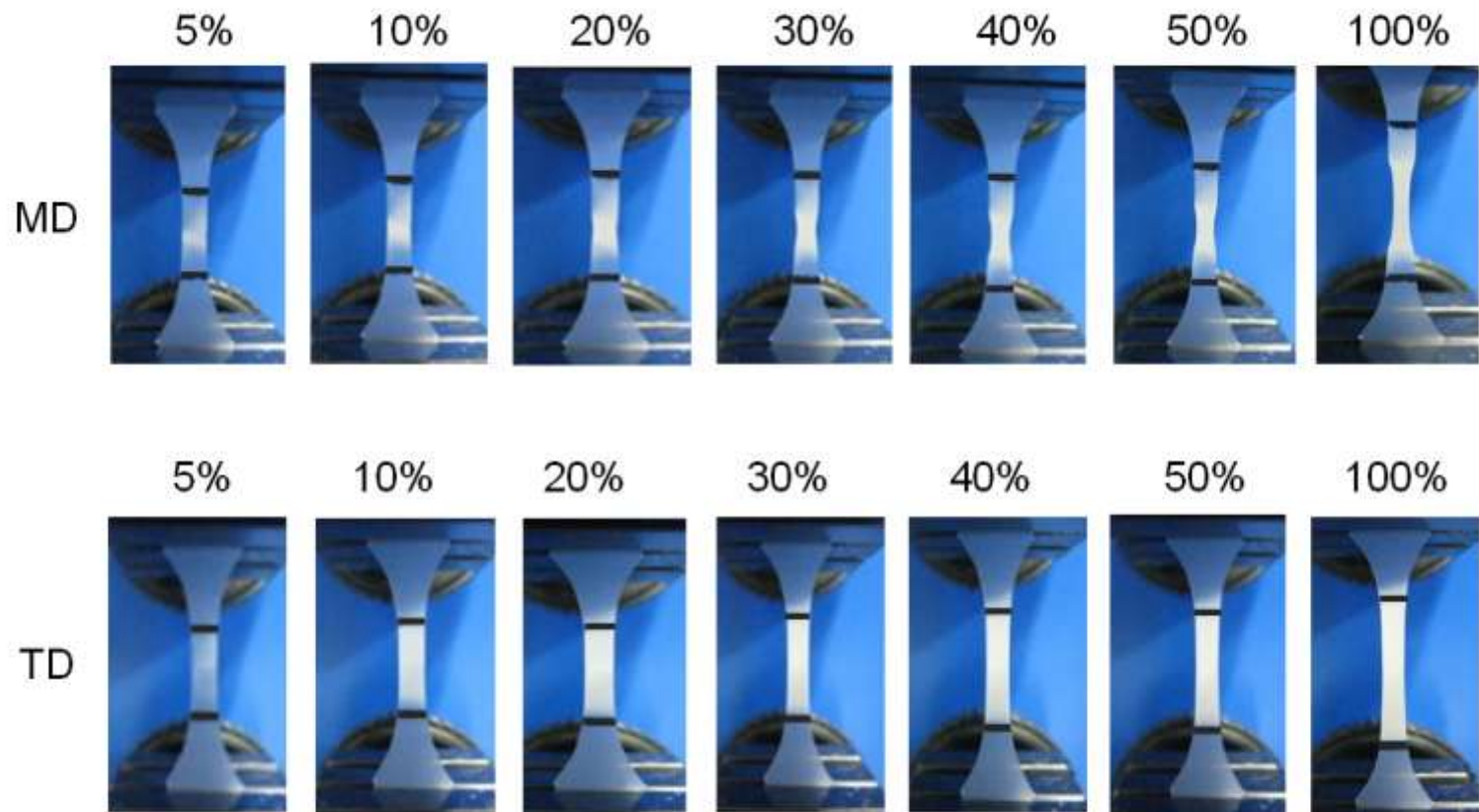


Figure 8 (b)